Iranian Journal of Materials Forming 13 (3) (2026) 26-33

IJMF

Online ISSN: 2383-0042

Iranian Journal of Materials Forming

Journal Homepage: http://ijmf.shirazu.ac.ir

Research Article

An Alternative Model for Investigating the Kinetics of Deformation-Induced Martensitic Transformation

Kimia Saberi Tavakoli and Hamed Mirzadeh*

School of Metallurgy and Materials Engineering, College of Engineering, University of Tehran, Tehran, Iran

ARTICLE INFO

Article history:

Received: 5 December 2025
Reviewed: 23 December 2025
Revised: 25 December 2025
Accepted: 28 December 2025

Keywords:

Metastable stainless steels
Plastic deformation
α'-martensite formation
Austenite stability
Phase transformation kinetics

Please cite this article as:

Saberi Tavakoli, K. & Mirzadeh, H. (2026). An alternative model for investigating the kinetics of deformation-induced martensitic transformation. *Iranian Journal of Materials Forming*, *13*(2), 26-33. https://doi.org/10.22099/IJMF.2025.55110.1365

ABSTRACT

Many austenitic stainless steels have a metastable austenite phase that transforms into α'-martensite during deformation at room and cryogenic temperatures. Given the significance of the deformation-induced martensitic transformation for strengthening, plasticity, and grain refinement, examining the kinetics of this transformation is an important issue. Accordingly, in the present work, an alternative kinetics model was introduced and verified by considering strain, deformation temperature, chemical composition, and strain rate as the main variables. This model was formulated as $f_{\alpha'} / f_{sat} = 1/\{1+1/(\lambda\varepsilon)^m\}$, where $f_{\alpha'}$ and f_{sat} represent the volume fraction of α′-martensite and its saturation value, respectively; ε is the equivalent strain, m was obtained as approximately 3 for the effect of deformation temperature and strain rate on α'-martensite formation in AISI 304 and AISI 301LN stainless steels, and λ was found to be a reliable metastability parameter. In the proposed model, λ and m can be determined without the need for non-linear regression, which is a clear advantage compared to other models. The proposed model was benchmarked against the well-known Olson-Cohen model, highlighting its advantages and confirming that it can serve as a viable option for future research works on austenitic stainless steels, advanced high-strength steels, and high-entropy alloys.

1. Introduction

Due to their remarkable corrosion resistance and mechanical properties, austenitic stainless steels are ideal materials for numerous engineering applications [1-3]. Many austenitic stainless steels have a metastable austenite phase that transforms into α'-martensite during deformation at room and cryogenic temperatures. This specific phase transformation results in significant strengthening effect [4, 5], improves plasticity via the transformation-induced plasticity (TRIP) effect during tensile deformation [6-8], and also enables significant grain refinement during subsequent controlled reversion/recrystallization annealing processes [9-12]. Given the significance of deformation-induced martensitic transformation, examining and tailoring the kinetics of this transformation is of considerable

* Corresponding author
E-mail address: hmirzadeh@ut.ac.ir (H. Mirzadeh)
https://doi.org/10.22099/IJMF.2025.55110.1365

importance [13]. The Olson-Cohen [14], Shin [15], Ahmedabadi [16], Tavares [17], and Hill-based [18] models are among the common ones that have been proposed. Each model has its own specific advantages and drawbacks. Additionally, it is important to connect the model parameters to the material properties and deformation conditions, a task that becomes difficult when considering the underlying mechanisms [18, 19]. Therefore, there is always a pressing need to introduce alternative models that can be simply applied.

The deformation-induced martensitic transformation is significantly affected by deformation variables, including the amount of deformation, deformation temperature [20, 21], strain rate [22, 23], and stress/strain states [24, 25]. Moreover, material parameters also significantly affect deformation-induced martensitic transformation, including the chemical composition and austenite grain size [26, 27]. Usually, these parameters impact the stacking fault energy (SFE) to affect the kinetics of deformation-induced martensitic transformation and the stability of austenite [28]. The deformation temperature is among the key variables that can be changed to tailor the kinetics of deformation-induced martensitic transformation.

Consequently, the present work seeks to tackle these concerns by introducing an alternative kinetics model, which will be verified by examining the effect of different parameters on α'-martensite formation kinetics in austenitic stainless steels.

2. Methodology

The Olson-Cohen model, based on Eq. (1) [14], is the most widely used equation for investigating the change in the volume fraction of α'-martensite ($f_{\alpha'}$) versus equivalent strain (ε):

$$f_{\alpha'} = 1 - exp\{-\beta\{1 - exp(-\alpha\varepsilon)\}^n\} \quad (1)$$

Where n is usually taken as 4.5 for austenitic stainless steels [14], α is associated with the shear-band formation rate, and β denotes the likelihood that a shear band intersection will produce an embryo [14]. Based on this model, α and β parameters can be obtained by non-linear fitting using plots of $f_{\alpha'}$ versus ε.

On the other hand, according to the idea of sigmoidal growth in mathematics, the equation of $y = y_0/\{1 + 1/(\lambda x)^m\}$ was considered, in which y_0, λ, and m are constants. By substituting $f_{\alpha'}$ instead of y and ε instead of x, the following equation can be obtained:

$$f_{\alpha'} = y_0/\{1 + 1/(\lambda\varepsilon)^m\} \quad (2)$$

At large ε, $f_{\alpha'}$ approaches its saturation value, meaning that $y_0 = f_{sat}$. Accordingly, Eq. (2) can be rewritten as Eq. (3), then as Eq. (4), and finally by taking the natural logarithm of both sides of Eq. (4), Eq. (5) can be obtained:

$$f_{\alpha'}/f_{sat} = 1/\{1 + 1/(\lambda\varepsilon)^m\} \quad (3)$$

$$f_{sat}/f_{\alpha'} - 1 = 1/(\lambda\varepsilon)^m \quad (4)$$

$$ln\{f_{sat}/f_{\alpha'} - 1\} = -m\,ln\,\lambda - m\,ln\,\varepsilon \quad (5)$$

Accordingly, the plot of $ln\{f_{sat}/f_{\alpha'} - 1\}$ versus $-ln\,\varepsilon$ can be fitted by a straight line with a slope of m and an intercept of $-m\ln\lambda$. In this way, it is possible to obtain λ and m without the need for non-linear regression.

As α'-martensite develops during plastic deformation, strain serves as the fundamental parameter. Additionally, deformation temperature, chemical composition, and strain rate are the key factors influencing the kinetics of martensitic transformation [20-23]. Thus, the impacts of strain, deformation temperature, chemical composition, and strain rate have been taken into account in this study for assessing the developed model. Nonetheless, it is important to note that stress/strain state [24, 25] and grain size [26, 27] may also influence the transformation kinetics. Moreover, besides austenitic stainless steels, the suitability of the model can be assessed for advanced high-strength steels and high-entropy alloys.

3. Results and Discussion

3.1. Olson-Cohen modeling

The relationship between transformation kinetics and

strain at various deformation temperatures (between −188 °C and 22 °C) has been obtained for AISI 304 stainless steel [14, 20], as illustrated in Fig. 1. It is evident that lowering the deformation temperature enhances the formation of α'-martensite, which is linked to a greater driving force and reduced SFE [19, 28]. The quicker accelerated kinetics of α'-martensite formation result in a reduced strain required to generate a notable quantity of α'-martensite, along with enhanced f_{sat}. In fact, decreasing the deformation temperature increases both the kinetics of α'-martensite formation and its final amount.

The curves related to the non-linear fitting by the Olson-Cohen model are also presented in Fig. 1. The Olson-Cohen model appears to be suitable for presenting the kinetics of α'-martensite formation. The sigmoidal nature of this equation is an important factor in this regard. On the other hand, the parameters of this model have physical meanings, and the acquired α and β values are presented in Fig. 2. It is observable that α diminishes with increasing in the deformation temperature. Given that α is influenced by SFE, it makes sense that α diminishes with increasing deformation temperature. In fact, by increasing the deformation temperature, the apparent SFE increases, which inhibits α'-martensite formation. Consequently, the trend of α evolution with deformation temperature aligns with the observed kinetics of α'-martensite formation. Reasonably, β also exhibits a consistent trend with increasing deformation temperature, except for the temperature range of −188 °C to −70 °C. Since β indicates the probability that an intersection of shear bands will generate a martensitic embryo, it can be concluded that increasing the deformation temperature is not conducive to the generation of martensitic embryos. Therefore, the Olson-Cohen model is a robust model, and its parameters have physical meanings. However, in this model, two main parameters are available, both of which vary with the main influencing parameter (here, deformation temperature). Moreover, it can be seen that β does not show a distinct trend for the whole deformation temperature range. These observations necessitate the introduction of alternative models.

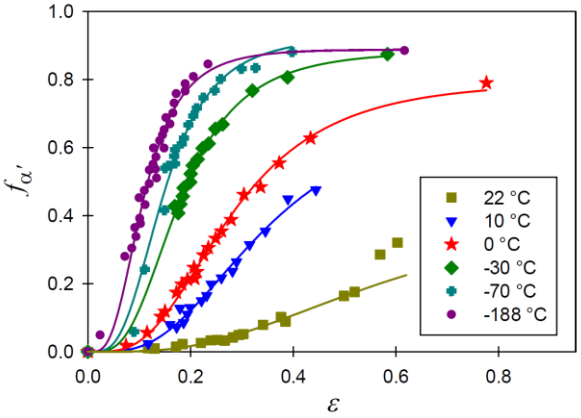

Fig. 1. Plots representing the kinetics of α'-martensite formation in AISI 304 stainless steel (data from [14, 20]) with the corresponding fitted Olson-Cohen curves in the present work.

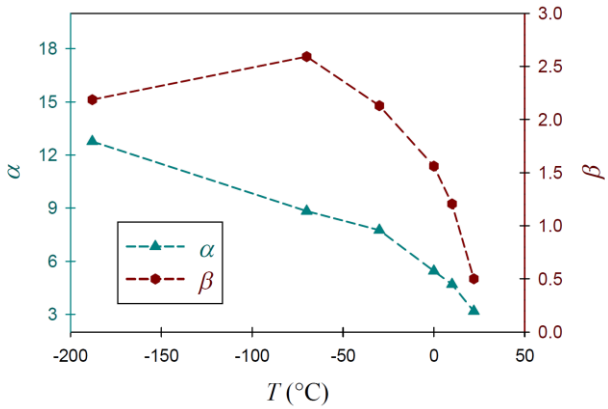

Fig. 2. Parameters of the Olson-Cohen model versus temperature based on the fittings of Fig 1.

Based on the curves obtained according to the Olson-Cohen model in Fig. 1, it is possible to estimate f_{sat} versus temperature for each deformation temperature. According to Eq. (1), at large ε, $exp(-\alpha\varepsilon)$ tends to zero, and hence, $f_{\alpha'}$ tends to $1-exp\{-\beta\}$. Therefore, f_{sat} can be estimated as follows:

$$f_{sat} = 1 - exp\{-\beta\} \quad (6)$$

Since β indicates the probability that an intersection of shear bands will generate a martensitic embryo, it is reasonable that the final amount of α'-martensite (f_{sat}) becomes dependent on the value of β. Based on the obtained values of β in Fig. 2, the values of f_{sat} were calculated, and the results are presented in Fig. 3. It can be seen that by increasing the deformation temperature, f_{sat} decreases significantly, indicating a severe inhibition of α'-martensite formation.

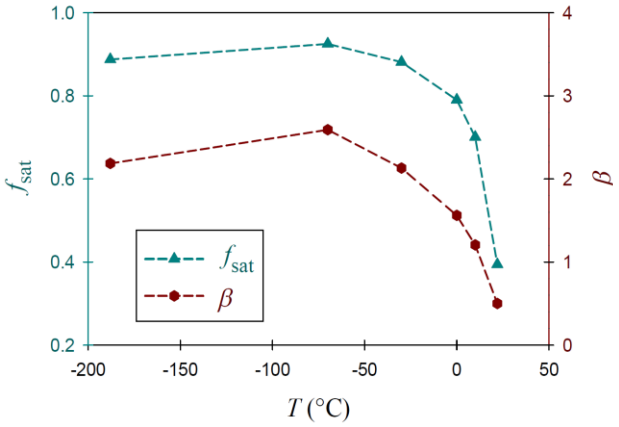

Fig. 3. f_{sat} and β versus deformation temperature.

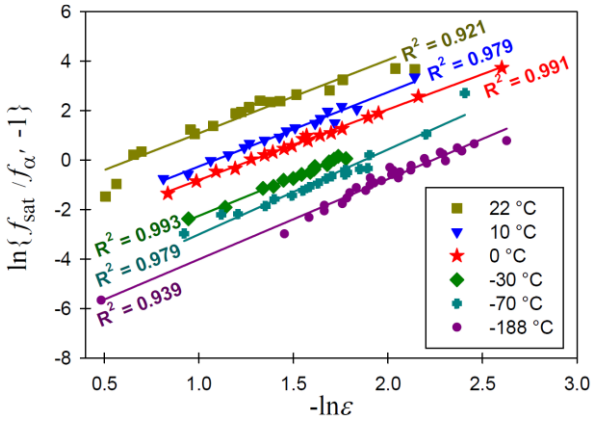

Fig. 4. Developed sigmoidal growth model applied to the results of AISI 304 stainless steel presented in Fig. 1.

3.2. Developed sigmoidal growth model

According to Eq. (5), the plot of $ln\{f_{sat}/f_{\alpha'}-1\}$ versus $-ln\,\varepsilon$ can be fitted by a straight line with a slope of m and an intercept of $-m\ln\lambda$. In this regard, the values of f_{sat} were taken from Fig. 3 and the corresponding plots for all deformation temperatures are depicted in Fig. 4. The existing data appear to align well with the fitted lines, indicating that the proposed model is suitable. This reveals that the developed model in Eq. (3) is suitable for representing the sigmoidal nature of α'-martensite formation, similar to the general trend seen for phase transformations in materials science [29].

Based on these analyses, the obtained values of m and λ are summarized in Fig. 5. It can be seen that the m values are near each other and can be averaged as ~3. This aspect can also be verified by considering of Fig. 4, where the fitted lines for all deformation temperatures are parallel, indicating a similar slope. It is an important advantage because the only parameter affected by the deformation temperature is λ. Fig. 5 reveals that λ is highly sensitive to the deformation temperature, and it decreases as the deformation temperature increases. Therefore, λ can be considered as the sole metastability parameter, indicating that increasing λ is conducive to α'-martensite formation kinetics. In addition, as shown in Fig. 5, it is possible to correlate λ with the deformation temperature. If the deformation temperature is expressed in degrees Celsius, the following equation can be obtained:

$$\lambda = 3.65 + 6.67 \times (1 - 0.99^{-T}) \quad (7)$$

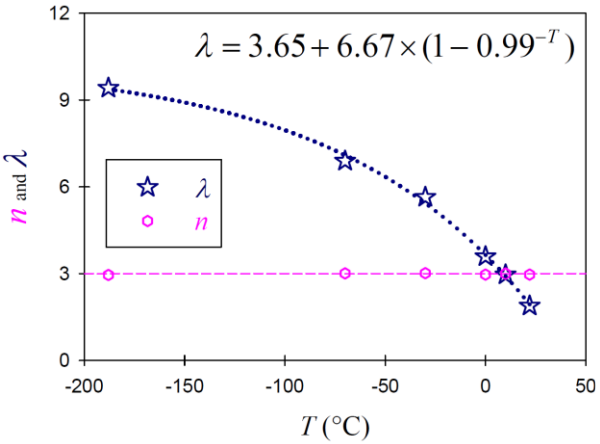

Fig. 5. Parameters of the developed sigmoidal growth model versus temperature based on the fittings of Fig. 4.

Based on Eq. (7), the temperature corresponding to λ = 0 can also be estimated as 43.4 °C. This reveals that by increasing the temperature to 43.4 °C, the metastability parameter λ tends to zero. Accordingly, α'-martensite formation becomes insignificant. This can be verified based on previous works [14, 20], where at ~ 50 °C, the amount of α'-martensite formed during tensile deformation became negligible. Therefore, it can be deduced that the developed model is a robust one for investigating α'-martensite formation kinetics.

In summary, for AISI 304 stainless steel, the developed model can be summarized as follows:

$$f_{\alpha'}/f_{sat} = 1/\{1 + 1/(\lambda\varepsilon)^m\}$$
$$m = 3 \quad (8)$$
$$\lambda = 3.65 + 6.67 \times (1 - 0.99^{-T})$$

3.3. Further verification of the proposed model

For further verification of the proposed model, the effects of the chemical composition and strain rate were

also considered. Regarding the chemical composition, AISI 304 and AISI 301LN stainless steels were compared, where the data for both alloys were taken from the work of Talonen and Hänninen [21]. According to Eq. (5), for each alloy, the plot of $ln\{f_{sat}/f_{\alpha'}-1\}$ versus $-ln\,\varepsilon$ was fitted by a straight line to find the values of m and λ. The corresponding plots are depicted in Fig. 6, resulting in m values of 3.040 and 3.098 for AISI 304 and AISI 301LN stainless steels, respectively. It can be seen that the value of m is still ~ 3, similar to the findings presented in Fig. 5. On the other hand, the λ values of 1.20 and 5.40 were calculated for AISI 304 and AISI 301LN stainless steels, respectively. It can be seen that the metastability parameter λ is much higher for AISI 301LN stainless steel, denoting a more pronounced kinetics for α'-martensite formation. This higher metastability is directly related to the chemical composition of AISI 301LN stainless steel. The change in chemical composition can be investigated based on the SFE of these stainless steels, which is 17.8 mJ/m^2 and 12.8 mJ/m^2 for AISI 304 and AISI 301LN stainless steels, respectively. Therefore, AISI 301LN stainless steel is more metastable, which can be verified based on both SFE and λ.

Regarding the effect of strain rate, the reported data for AISI 301LN stainless steel from the work of Talonen and Hänninen [21] were considered, as depicted in Fig. 7(a). It can be seen that for strain rates of 0.0003 s^{-1}, 0.1 s^{-1}, and 200 s^{-1}, the m values were obtained as 3.098, 3.073, and 3.061, respectively. It can be seen that the value of m is still ~ 3, similar to the findings presented in Fig. 5 and 6. On the other hand, the λ values of 5.40, 4.62, and 3.98 were calculated for strain rates of 0.0003 s^{-1}, 0.1 s^{-1}, and 200 s^{-1}, respectively. It can be seen that the metastability parameter λ decreases as the strain rate increases, as summarized in Fig. 7(b), which denotes slower α'-martensite formation kinetics. This effect has primarily been correlated to the adiabatic heating effect at higher strain rates, which reduces the driving force for α'-martensite formation [30, 31]. In this regard, however, Talonen and Hänninen [21] showed that the temperature dependence of the SFE could be the crucial factor in inhibiting the transformation at higher strain rates.

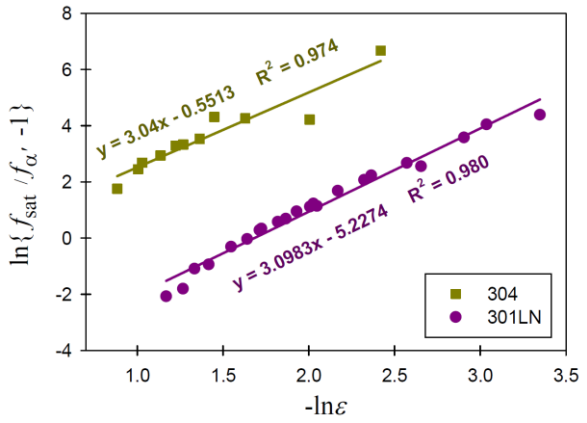

Fig. 6. Developed sigmoidal growth model applied to the results of AISI 304 and 301LN stainless steels tensile deformed at room temperature with a strain rate of 0.0003 s^{-1} (data from [21]).

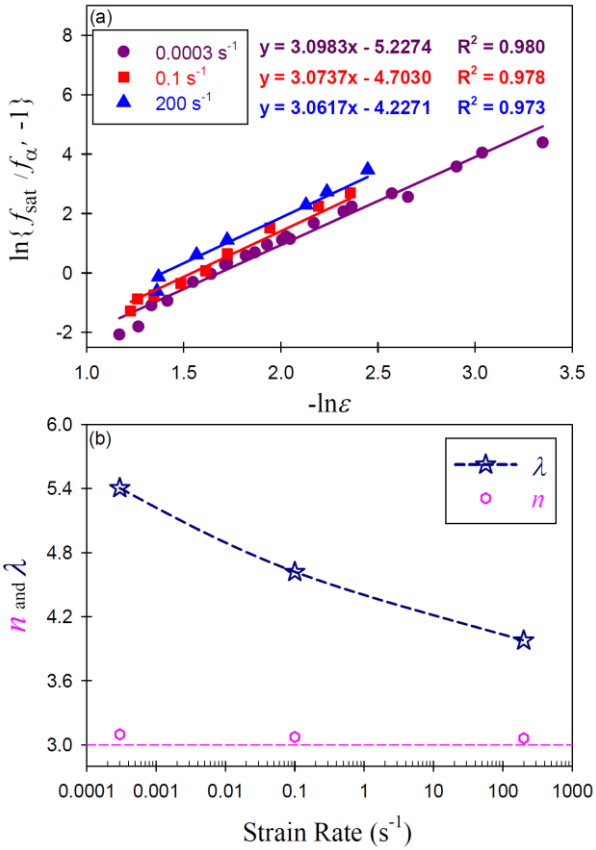

Fig. 7. (a) Developed sigmoidal growth model applied to the results of AISI 301LN stainless steel tensile deformed at room temperature with various strain rates (data from [21]), where a few data points with high discrepancy have been removed and, (b) parameters of the developed sigmoidal growth model versus strain rate.

The above findings reveal that the proposed model is capable of investigating α'-martensite transformation kinetics and the main parameter of this model (λ) is meaningful and represents the degree of metastability. This model is appropriate for comparison purposes

based on the obtained values of λ. Therefore, this simple model can be used in future investigations to represent the effects of other deformation conditions, as well as the effect of chemical composition of the material and its average grain size.

4. Conclusions

In this work, an alternative model was introduced and evaluated for investigating α′-martensite formation kinetics, which is formulated as $f_{\alpha'}/f_{sat} = 1/\{1+1/(\lambda\varepsilon)^m\}$. Moreover, it was also compared with the well-known Olson-Cohen model. Accordingly, the following conclusions can be drawn:

(1) The plot of $ln\{f_{sat}/f_{\alpha'}-1\}$ versus $-ln\,\varepsilon$ can be fitted by a straight line with slope m and intercept -$m$lnλ. This allows λ and m to be determined without non-linear regression, which is an important advantage over the competing models.

(2) λ was found as a reliable metastability parameter, sensitive to the deformation temperature, strain rate, and chemical composition. The parameter m can be considered approximately constant (~3), leaving λ as the main variable reflecting material metastability.

(3) Investigating the effect of deformation temperature (T, °C) on α'-martensite formation in AISI 304 stainless steel resulted in $\lambda = 3.65 + 6.67 \times (1 - 0.99^{-T})$.

(4) Comparison of AISI 304 and AISI 301LN stainless steels shows λ values of 1.20 and 5.40, respectively. The effect of the chemical composition was correlated to SFE of the studied stainless steels.

(5) For AISI 301LN, λ values of 5.40, 4.62, and 3.98 were obtained at strain rates of 0.0003 s^{-1}, 0.1 s^{-1}, and 200 s^{-1}, respectively. This confirms that metastability decreases at higher strain rates.

Conflict of interest

The authors declare no conflict of interest.

Author's Contributions

Kimia Saberi Tavakoli: *Investigation, Writing - original draft*

Hamed Mirzadeh: *Conceptualization, Supervision, Writing - review & editing*

Funding

This work received no funding.

5. References

[1] Mirzaei, M., & Paydar, M. H. (2019). Anisotropy in elastic properties of porous 316L stainless steel due to the shape and regular cell distribution. *Iranian Journal of Materials Forming, 6(1)*, 56–63. https://doi.org/10.22099/ijmf.2019.31703.1117

[2] Muñoz, J. A., Dolgach, E., Tartalini, V., Risso, P., Avalos, M., Bolmaro, R., & Cabrera, J. M. (2023). Microstructural heterogeneity and mechanical properties of a welded joint of an austenitic stainless steel. *Metals, 13(2)*, 245. https://doi.org/10.3390/met13020245

[3] Bagherpour, E., Reihanian, M., Pardis, M., Ebrahimi, R., & Langdon, T. G. (2018). Ten years of severe plastic deformation (SPD) in Iran, part I: Equal-channel angular pressing (ECAP). *Iranian Journal of Materials Forming, 5(1)*, 71–113. https://doi.org/10.22099/IJMF.2018.28756.1101

[4] Li, J., Cheng, W., Qin, W., Chen, M., Zhao, Y., Li, Y., Mao, Q. (2023). Cryogenic impact property of a high-strength-ductility 304L stainless steel with heterogeneous lamella structure. *Journal of Materials Research and Technology, 24*, 1401–1409. https://doi.org/10.1016/j.jmrt.2023.03.081

[5] Kishore, K., Kumar, R. G., & Chandan, A. K. (2021). Critical assessment of the strain-rate dependent work hardening behaviour of AISI 304 stainless steel. *Materials Science and Engineering: A,* 803, 140675. https://doi.org/10.1016/j.msea.2020.140675

[6] Jalali, A., Mehranpour, M. S., Kalhor, A., Sohrabi, M. J., Heydarinia, A., Hasnabadi, F., Mirzadeh, H., Malekan, M., Sarkari Khorrami, M., Fallah, V., & Rodak, K. (2025). Superior strength-ductility synergy in metastable high-entropy alloys: the crucial role of FCC to BCC martensitic phase transformation. *Journal of Alloys and Compounds, 1044*, 184464. https://doi.org/10.1016/j.jallcom.2025.184464

[7] Khorrami, M., Hanzaki, A. Z., Abedi, H. R., Moallemi, M., Mola, J., & Chen, G. (2021). On the effect of Mn-content on the strength-ductility balance in Ni-free high N transformation induced plasticity steels. *Materials Science and Engineering: A, 814*, 141260. https://doi.org/10.1016/j.msea.2021.141260

[8] Zadeh, S. H., Jafarian, H. R., Park, N., & Eivani, A. R. (2020). Regulating of tensile properties through microstructure engineering in Fe-Ni-C TRIP steel processed by different strain routes of severe deformation. *Journal of Materials Research and Technology, 9(3)*, 2903–2913. https://doi.org/10.1016/j.jmrt.2020.01.041

[9] Eskandari, M., Khosravi, B. I., Alavi, Z. S. R., & Yeganeh, M. (2022). Effect of cold-rolling and annealing treatments on the microstructure and mechanical properties of AISI 309S austenitic stainless steel. *Iranian Journal of Materials Forming, 9(3)*, 52–61. https://doi.org/10.22099/IJMF.2022.43813.1228

[10] Qin, W., Li, J., Liu, Y., Kang, J., Zhu, L., Shu, D., Peng, P., She, D., Meng, D., & Li, Y. (2019). Effects of grain size on tensile property and fracture morphology of 316L stainless steel. *Materials Letters, 254*, 116–119. https://doi.org/10.1016/j.matlet.2019.07.058

[11] Behjati, P., Kermanpur, A., Najafizadeh, A., Samaei Baghbadorani, H., Karjalainen, L. P., Jung, J. G., & Lee, Y.-K. (2014). Effect of nitrogen content on grain refinement and mechanical properties of a reversion-treated Ni-free 18Cr-12Mn austenitic stainless steel. *Metallurgical and Materials Transactions A, 45(13)*, 6317–6328. https://doi.org/10.1007/s11661-014-2595-4

[12] Hamada, A. S., Kisko, A. P., Sahu, P., & Karjalainen, L. P. (2015). Enhancement of mechanical properties of a TRIP-aided austenitic stainless steel by controlled reversion annealing. *Materials Science and Engineering: A, 628*, 154–159. https://doi.org/10.1016/j.msea.2015.01.042

[13] Jain, A., & Varshney, A. (2024). A critical review on deformation-induced transformation kinetics of austenitic stainless steels. *Materials Science and Technology, 40(2)*, 75–106. https://doi.org/10.1177/02670836231212618

[14] Olson, G. B., & Cohen, M. (1975). Kinetics of strain-induced martensitic nucleation. *Metallurgical transactions A, 6(4)*, 791–795. https://doi.org/10.1007/BF02672301

[15] Shin, H. C., Ha, T. K., & Chang, Y. W. (2001). Kinetics of deformation induced martensitic transformation in a 304 stainless steel. *Scripta Materialia, 45(7)*, 823–829. https://doi.org/10.1016/S1359-6462(01)01101-0

[16] Ahmedabadi, P. M., Kain, V., & Agrawal, A. (2016). Modelling kinetics of strain-induced martensite transformation during plastic deformation of austenitic stainless steel. *Materials & Design, 109*, 466–475. https://doi.org/10.1016/j.matdes.2016.07.106

[17] Tavares, S. S. M., Pardal, J. M., Da Silva, M. J. G., Abreu, H. F. G. de, & da Silva, M. R. (2009). Deformation induced martensitic transformation in a 201 modified austenitic stainless steel. *Materials Characterization, 60(8)*, 907–911. https://doi.org/10.1016/j.matchar.2009.02.001

[18] Sohrabi, M. J., Mehranpour, M. S., Heydarinia, A., Kalhor, A., Lee, J. H., Mirzadeh, H., Mahmudi, R., Parsa, M. H., Rodak, K., & Kim, H. S. (2024). Deformation-induced martensitic transformation kinetics in TRIP-assisted steels and high-entropy alloys. *Acta Materialia, 280*, 120354. https://doi.org/10.1016/j.actamat.2024.120354

[19] Lo, K. H., Shek, C. H., & Lai, J. K. L. (2009). Recent developments in stainless steels. *Materials Science and Engineering: R: Reports, 65(4–6)*, 39–104. https://doi.org/10.1016/j.mser.2009.03.001

[20] Angel, T. (1954). Formation of martensite in austenitic stainless steels effects of deformation, temperature, and composition. J. *Iron and Steel Inst, 177*, 165–174. https://doi.org/10.1299/kikaia.72.1561

[21] Talonen, J., & Hänninen, H. (2007). Formation of shear bands and strain-induced martensite during plastic deformation of metastable austenitic stainless steels. *Acta Materialia, 55(18)*, 6108–6118. https://doi.org/10.1016/j.actamat.2007.07.015

[22] Dan, W. J., Zhang, W. G., Li, S. H., & Lin, Z. Q. (2007). A model for strain-induced martensitic transformation of TRIP steel with strain rate. *Computational Materials Science, 40(1)*, 101–107. https://doi.org/10.1016/j.commatsci.2006.11.006

[23] Talonen, J., Hänninen, H., Nenonen, P., & Pape, G. (2005). Effect of strain rate on the strain-induced γ→ α′-martensite transformation and mechanical properties of austenitic stainless steels. *Metallurgical and Materials Transactions A, 36(2)*, 421–432. https://doi.org/10.1007/s11661-005-0313-y

[24] Iwamoto, T., Tsuta, T., & Tomita, Y. (1998). Investigation on deformation mode dependence of strain-induced martensitic transformation in trip steels and modelling of transformation kinetics. *International Journal of Mechanical Sciences, 40(2–3)*, 173–182. https://doi.org/10.1016/S0020-7403(97)00047-7

[25] Polatidis, E., Haidemenopoulos, G. N., Krizan, D., Aravas, N., Panzner, T., Šmíd, M., Papadioti, I., Casati, N., Van Petegem, S., & Van Swygenhoven, H. (2021). The effect of stress triaxiality on the phase transformation in transformation induced plasticity steels: Experimental investigation and modelling the transformation kinetics. *Materials Science and Engineering: A, 800*, 140321. https://doi.org/10.1016/j.msea.2020.140321

[26] Sohrabi, M. J., Mirzadeh, H., Sadeghpour, S., & Mahmudi, R. (2023). Grain size dependent mechanical behavior and TRIP effect in a metastable austenitic stainless steel. *International Journal of Plasticity, 160*, 103502. https://doi.org/10.1016/j.ijplas.2022.103502

[27] Jung, Y.-S., Lee, Y.-K., Matlock, D. K., & Mataya, M. C. (2011). Effect of grain size on strain-induced martensitic transformation start temperature in an ultrafine grained metastable austenitic steel. *Metals and Materials International, 17(4)*, 553–556. https://doi.org/10.1016/j.scriptamat.2008.02.024

[28] Sohrabi, M. J., Naghizadeh, M., & Mirzadeh, H. (2020). Deformation-induced martensite in austenitic stainless steels: A review. *Archives of Civil and Mechanical Engineering, 20(4)*, 124. https://doi.org/10.1007/s43452-020-00130-1

[29] Porter, D. A., & Easterling, K. E. (2009). Phase transformations in metals and alloys (revised reprint). CRC Press. https://doi.org/10.1201/9781439883570

[30] Murr, L. E., Staudhammer, K. P., & Hecker, S. S. (1982). Effects of strain state and strain rate on deformation-induced transformation in 304 stainless steel: Part II. Microstructural study. *Metallurgical Transactions A, 13(4)*, 627–635. https://doi.org/10.1007/BF02644428

[31] Ferreira, P. J., Vander Sande, J. B., Fortes, M. A., & Kyrolainen, A. (2004). Microstructure development during high-velocity deformation. *Metallurgical and Materials Transactions A, 35(10)*, 3091–3101. https://doi.org/10.1007/s11661-004-0054-3